

Development of Vision-based Autonomous Robotic Fish and Its Application in Water-polo-attacking Task

Wei Zhao, Yonghui Hu, Guangming Xie, Long Wang, and Yingmin Jia

Abstract—This paper presents the design and locomotion control of a vision-based autonomous robotic fish, and its application in water-polo-attacking task. Most of previous work on task strategies of autonomous robots is focused on the terrestrial robots and seldom deals with underwater applications. In fact, the tasks in underwater environment are more challenging than those in ground circumstances due to the uncertainties and complexity in hydro-environment. In this paper, a water-polo-attacking task is designed and implemented based on artificial potential field. The experimental results are presented to verify the effectiveness of the proposed control algorithms.

I. INTRODUCTION

Compared with propeller-driven underwater vehicles, fish achieve far superior swimming performance, such as high efficiency, great agility, station keeping ability and perfect signature reduction. Taking advantage of recent progress in robotics, control technology, artificial intelligence, hydrodynamics of fish-like swimming, new materials, sensors, and actuators, emerging research has focused on developing novel fish-like vehicles, aiming to incorporate biological principles into engineering practice.

However, most of previous robotic fish projects were focused on the propulsion mechanism of fish swimming, the mechanical structures and the motion control. In 1994 at MIT, Triantafyllou *et al.* pioneered the study of robotic fish by developing the well-known RoboTuna that propels with posterior flexible body and oscillating tail foils [1], [2]. Mason *et al.* constructed a three-link carangiform swimmer for prediction of thrust generation with flapping tail [3]. Liu *et al.* developed autonomously swimming robotic fish based on biologically inspired behavior-based approach [4]. Kato *et al.* developed a pectoral fin driven robotic fish called “BlackBass” for precise maneuvering control [5].

Developing systems for autonomous robotic fish to address complex tasks is particularly challenging. An autonomous robotic fish needs to perceive its environment, make decisions about selection of its actions, and finally carry out its actions. However, most of the success stories in task performance of autonomous robots are obtained in the terrestrial field. For the underwater case, results are relatively few. This is because the hydro-environment is more complicated than ground environments and has many different sources of

uncertainty. When exploiting ocean resources, autonomous underwater robot system can undoubtedly provide a convenient and low-cost solution to access the ocean. Thus, research on task performance of autonomous underwater robots becomes more and more necessary and significant.

In this paper, a vision-based autonomous robotic fish is presented and applied in a water-polo-attacking task. The contributions of this paper are twofold: first, a type of autonomous robotic fish with onboard camera is designed and its motion control is realized with a sinusoidal CPG model; second, it is applied in a water-polo-attacking task and the problem of path planning and obstacle avoidance is investigated based on artificial potential field. Specifically, the procedures and algorithms for underwater vision processing are proposed and the effect is given. The autonomous robotic fish shows great promise of utility in practical applications such as seabed exploration, oilpipe leakage detection, oceanic supervision, military detection, and so on.

The rest of the paper is organized as follows. In Section II, design details including the mechanical structure and electronic system are described. In Section III, the CPG model and its application to the locomotion control of the autonomous robotic fish are presented, and several swimming gaits involving movements of the tail and pectoral fins are designed. Section IV presents the algorithms for underwater vision processing. In Section V, a water-polo-attacking task is designed and the control strategies by combination of PD controller and artificial potential field approach are proposed. Section VI describes the experimental results. Finally, Section VII concludes the paper and summarizes the future work.

II. ROBOT DESIGN

A. Mechanical Design

The robotic fish is composed of several elements: a rigid main body, a tail fin, two pectoral fins. The main body is a streamlined, waterproofed hull made of fiberglass and provides housings for the power, electronics and actuators. The robotic fish has three degrees of freedom (DOFs) with one for the tail fin and two for the pectoral fins. The actuators that drive all DOF are Hitec HS-5955TG servomotors. The servomotors are fixed on the bottom cover that is screwed to the main body with O-rings between them and the rotations of the servomotors are transmitted to the outside through dynamic sealing structure. The rotation range of the tail fin is limited to $\pm 90^\circ$, while that of the pectoral fins are expanded to $\pm 180^\circ$ with gear sets of 1 : 2 ratio for 3-D swimming of the robotic fish. On top of the main body are the power switch,

This work was supported by NSFC (60674050 and 60528007), National 973 Program (2002CB312200), and 11-5 project (A2120061303).

W. Zhao, Y. Hu, G. Xie, and L. Wang are with Intelligent Control Laboratory, Department of Mechanics and Space Technologies, College of Engineering, Peking University, Beijing 100871, China. email: zhaowei@june@gmail.com.

Y. Jia is with the Seventh Research Division, Beijing University of Aeronautics and Astronautics, Beijing 100083, P. R. China.



Fig. 1. Prototype of the autonomous robotic fish.

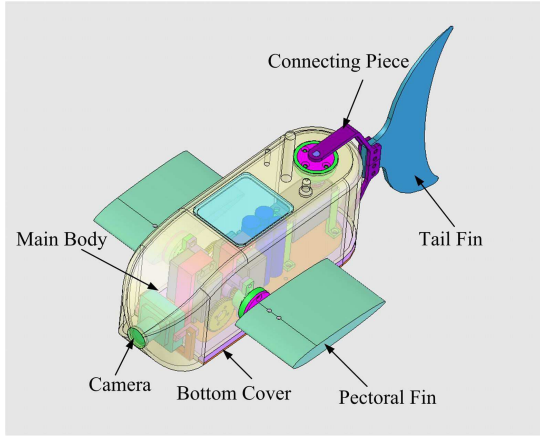


Fig. 2. 3-D model of the autonomous robotic fish.

antenna and recharge plug. A CMOS camera is installed at the mouth position with a transparent window glued to the hull for waterproof purpose. The density of the robotic fish has been designed to be close to that of water through careful calculations, so that little trimming weight or foam can be added to accomplish neutral buoyancy. Fig. 1 shows the photograph of the robotic fish prototype and the 3-D model of the robotic fish is illustrated in Fig. 2.

B. Electronic Design

The robotic fish is designed for autonomous operation such that it is equipped with onboard power, embedded processor, image sensor, and a duplex wireless communication module. Four rechargeable Ni-Cd cells of 2700 mAh capacity provide the robotic fish about one hour power autonomy. The control unit is a microcontroller S3C2440 that incorporates a high-performance 32-bit RISC, ARM920T CPU core running at 400 MHz and a wide range of peripherals from Samsung Electronics. The microcontroller captures image data in YCbCr 4:2:2 format from onboard camera at 320 × 240

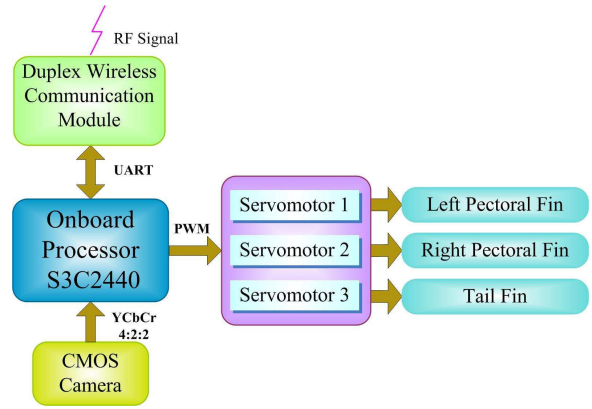


Fig. 3. Hardware architecture of control system.

resolution and does real-time image processing for perception of the environment. The microcontroller also does decision-making and generates three PWM signals to control the movements of the joints. The servomotor has internal position feedback and the degree of the turn of the axis depends upon the input PWM (Pulse Width Modulation) signal. Fig. 3 illustrates hardware architecture of the control system.

Finally, Table I summarizes the basic technical parameters of this autonomous robotic fish prototype.

III. LOCOMOTION CONTROL

A. CPG-based Motion Control

Central Pattern Generators (CPGs), which generate fundamental rhythmic movements in locomotion, such as walking, running, swimming and flying, can be used to produce the swimming motion of the robotic fish [6]–[8]. The locomotion controller consists of a CPG model for generating coordinated gait patterns. To reduce the computational complexity, a simple sinusoidal CPG model is employed here. The angular value of each rotating joint can be described by the following equation:

$$\theta_i(t) = \bar{\theta}_i + A_i \sin(2\pi f_i t + \phi_i) \quad (i = 1, 2, 3) \quad (1)$$

TABLE I
TECHNICAL PARAMETERS OF THE AUTONOMOUS ROBOTIC FISH
PROTOTYPE.

ITEM	VALUE
Dimension (L × W × H)	~350 mm × 80 mm × 120 mm
Weight	~1.5 kg
Number of tail joints	1
Number of pectoral fins	2
Power supplying	DC, 4.8 V, 2700 mAh
Microcontroller	S3C2440
Actuator mode	R/C Servomotor
Operation mode	Radio Control, 444 MHz
Sensor	Camera C3188A

where $\theta_i(t)$ is the angular position of the i -th joint at time t , $\bar{\theta}_i$ denotes the angular offset, A_i represents the oscillatory amplitude of the joint angle, and f_i indicates the frequency. The swimming speed of the robotic fish can be adjusted by modulating the value of the frequency f and the amplitude A . The angular offset $\bar{\theta}$ can be used as a strategy for maneuvering and three-dimensional swimming of the robotic fish.

B. Typical Swimming Gaits

Fish in nature exhibit various swimming movements that can be classified into periodic swimming and transient swimming. The periodic swimming is characterized by a cyclic repetition of the propulsive movements for a long distance, while the transient swimming includes fast start, escape maneuvers and turns [9].

Both the tail fin and the pectoral fins of the robotic fish can generate propulsion and maneuvering forces and combined to produce a great diversity of swimming gaits through the coordinated control. Based upon the propulsors used, the swimming can be classified into two basic modes: BCF (body and/or caudal fin) mode and MPF (median and/or paired fin) mode, although the combined use of tail and pectoral fins can produce more complex movements. The following typical swimming gaits have been designed and implemented on the robotic fish:

1) **BCF Forward Swimming:** The robotic fish swims in a straight line by actuating the tail fin, while the pectoral fins are held parallel to the horizontal plane functioning to enhance stability.

2) **BCF Turning in Advancing:** The angular offset is superimposed on the oscillation of the tail joint while other parameters remain the same as the BCF forward swimming. The tail not only provides the thrust but also produces a nonzero time-averaged torque that will cause a change in heading direction.

3) **MPF Forward and Backward Swimming:** The swimming gaits can be achieved by the synchronized oscillations of the paired pectoral fins around the horizontal plane, with caudal fin held straight. The angular offsets $\bar{\theta}$ of pectoral fin actuators determine the swimming direction.

4) **MPF Turning:** The differentiation of hydrodynamic forces between the pectoral fins will cause a yawing moment that is necessary to execute turning maneuvers on the fish body. An effective method to produce the yawing moment is to produce anteriorly directed force on one side and posteriorly directed force on the other side. Another method is with both pectoral fins flapping forward/backward and the tail fin as a rudder.

5) **Submerging and Ascending:** The robotic fish achieve three-dimensional motion by adjusting the attack angle of the pectoral fins like sharks that do not have swim bladders. As a precondition, the robotic fish should attain a higher swimming speed with BCF or MPF forward swimming gait. The inclined pectoral fin will cause a force that can be analyzed into a drag component and a positive or negative lift component. Another method for up-and-down motion is

with the pectoral fins oscillating synchronously around the vertical plane functioning to generate lift forces.

6) **Braking:** To accomplish a braking, fish generate an anteroventrally directed jet by synchronously moving the pectoral fins rapidly out from the body. The robotic fish brakes through sudden rotation of the pectoral fins to a position perpendicular to the body. The drag caused by the pectoral fin decelerates and eventually stops the motion of the robotic fish.

IV. VISION

The vision system is responsible for extracting interested information from the camera that is the only exteroceptive sensor of the robotic fish. The vision processing is based on color information, where the images are digitized in YCbCr color space, and color thresholds that were learned offline are then applied to the image. However, the aquatic environment imposes many negative influences on the quality of the images, such as poor visibility, ambient light, frequency-dependent scattering and absorption both between the camera and the environment, so that the processing method has to be adaptive and robust. Inspired by robotic soccer [10]–[12], the following steps are carried out in vision processing.

A. Color Segmentation

The robotic fish uses a 3-D lookup table to perform the mapping from YCbCr pixel values to symbolic color class. The lookup table is indexed by the raw Y, Cb, and Cr values of the pixel. Each entry of the lookup table stores the index number for the symbolic color to assign to the pixel, otherwise set to 0 if the pixel is background. The thresholds are learned from example images offline. The color segmentation process uses the threshold table on each pixel of the image to classify the image. Fig. 4 shows the effect of the color segmentation.

B. Pixel Connection and Region Merging

After the color segmentation process, the vision system then carries out the following steps: pixel connection and region merging. The connection procedure scans adjacent rows and merges runs (horizontal neighboring pixels of the same color) to make a region. The statistics gathered for a region include: bounding box, centroid, and area. The region merging process is done with the calculation of the region's

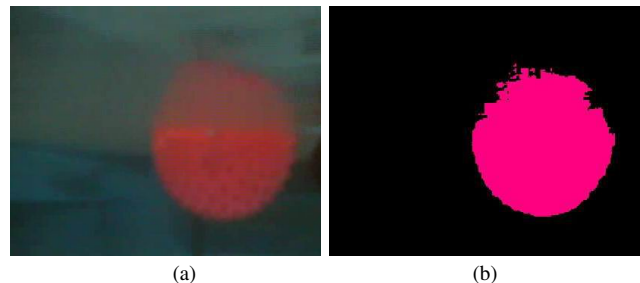


Fig. 4. (a) Sample underwater image of a water polo from the robotic fish's camera. (b) Image after color thresholding.

statistic characteristics. The criterion for deciding to merge the regions is the resulting density of the combined region. Two regions are combined into one region if the combined pixel area has a density occupying the area of new bounding box above a threshold for that color class. The purpose of region merging is to combine several nearby smaller regions of the same color into a single larger region in order to identify object and remove noise.

C. Feature Extraction of Objects

Using the regions determined by above procedures, the interested information of objects in the camera image can be extracted and the position of these objects relative to the robotic fish can also be estimated. With water-polo-attacking task (see next Section) taken into consideration, the processing strategies for feature extraction of each object are as follows:

1) *Water Polo*: The water polo is a pink spherical object, so it can be detected as a pink circular region on the image plane. The centroid of the water polo is regarded as the centroid of the pink region. The distance of the robotic fish to the water polo is determined by similar triangles: the preknown radius of the water polo divided by the distance is equal to the pixel radius on the image divided by the focal distance.

2) *Goal*: The goal is located between left half gate and right half gate marked with bright green color. The two half gates are then detected as two large bright green quadrate regions on the image. The centroid of the goal is considered as the center between the leftmost point of the right large green region and the rightmost point of the left large green region. The distance of the robotic fish to the goal is also determined by triangulation based on the height of the green marker of the gates.

3) *Obstacles*: The obstacles are two field green objects, one is cylinder-shaped, and the other is cubic. The resulting image on the image plane is two colored regions that are approximately quadrate. The distance of the robotic fish to the obstacle is calculated by triangulation similarly.

V. APPLICATION IN WATER-POLO-ATTACKING TASK

A. Task Description

In this section, we demonstrate the autonomous robotic fish with a water-polo-attacking task, which is a subtask in RoboFish-Cup competition that might be a standard competition of RoboCup in future. In a quadrate tank, there are an autonomous robotic fish, a water polo, two static obstacles, and a goal located between two half gates. In the task, the autonomous robotic fish tries to push the water polo into the goal with obstacle avoidance. The playing field for the robotic fish is a swimming tank of 225 cm in length and 125 cm in width. The goal with 30 cm wide is centered on one end of the field. Fig. 5 shows a sketch of the playing field for water-polo-attacking of the autonomous robotic fish.

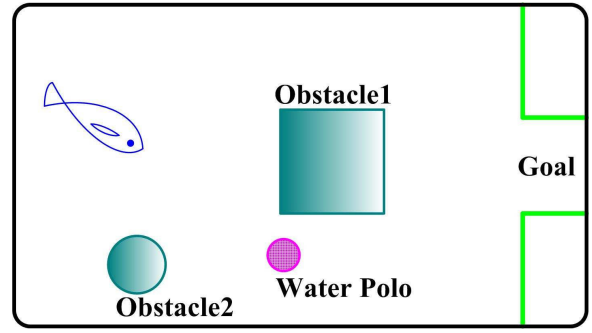


Fig. 5. Playing field for water-polo-attacking of the autonomous robotic fish.

Compared with the ground circumstance for robotic soccer, the hydro-environment is more complicated and uncertain, which makes the attacking task more difficult to achieve.

B. Control Strategies

The water-polo-attacking task is decomposed into two following subtasks: (1) water-polo-tracking, and (2) path planning and obstacle avoidance. A proportional-derivative (PD) controller is adopted to achieve water-polo-tracking, while an artificial potential field (APF) approach is presented for path planning and obstacle avoidance.

1) *Water-polo-tracking Based on PD Controller*: For the autonomous robotic fish with onboard vision sensor, the error signal is defined as the Euclidean distance between the centroid of the target (water polo) region and the center of the image frame (i.e. the center of the camera's field of view). Two error signals in the xy axis of image coordinates are used for pitch and yaw, and both these signals can then be propagated to the PID controller. For simplicity, the controller for water-polo-tracking is designed as a PD controller that takes the error signals from the autonomous robotic fish and produces pitch and yaw commands for the gait generator. Given the input from the robotic fish at any instant, and the previous robotic fish inputs, the controller generates commands based on the following control law:

$$\mu_i = K_p \bar{\epsilon}_i + K_d \frac{\partial \bar{\epsilon}_i}{\partial t} \quad (2)$$

The discrete form of (2) is expressed as follows:

$$\mu_i = K_p \bar{\epsilon}_i + \frac{K_d}{T} (\bar{\epsilon}_i - \bar{\epsilon}_{i-1}) \quad (3)$$

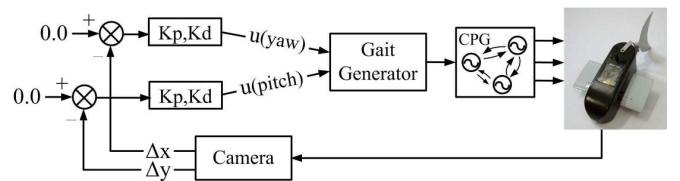


Fig. 6. Vision-based tracking control loops for the autonomous robotic fish. The 0.0 inputs represent the desired location of the target (water polo), corresponding to the center of the camera's field of view relative coordinate.

where K_p and K_d are respectively the proportional and differential gains, T denotes the sample period, $\bar{\varepsilon}_i$ is the time-averaged error signal at the i -th time and is defined recursively as:

$$\bar{\varepsilon}_i = \varepsilon_i + \gamma \bar{\varepsilon}_{i-1} \quad (4)$$

where ε_i is the error signal at the i -th time, and γ is the error propagation constant.

In order to track the water polo, the robotic fish tries to maintain the target in the center of its camera's field of view, where two feedback loops are necessary as shown in Fig. 6. Yaw commands are used to correct error in the image's x-axis, while pitch commands in the y-axis.

2) *Path Planning and Obstacle Avoidance Based on APF*: The artificial potential field method is widely used for path planning and obstacle avoidance of autonomous mobile robot due to its simplicity and mathematical elegance. The APF uses two types of potential field, namely a repulsive potential field to force a robot away from obstacles and an attractive potential field to drive the robot to its goal [13]–[15]. These potentials are added to form a composite potential to steer the robot. In contrast to controlling ground mobile robots, it is more difficult to modulate the attitudes of robotic fish due to the particularity of the aquatic environment as well as the uniqueness of the locomotion mode for robotic fish. This APF-based method, after some adaptations, can be applied in path planning and obstacle avoidance of the autonomous robotic fish.

Utilizing APF, two basic behaviors are designed in this subtask: move-to-goal behavior and avoid-obstacle behavior. Here, a behavior represents action or action sequence with intention. The behavior is a reaction to some stimulus from the environment, or a way of acting. For the robotic fish, an action means a gait sequence, which can be obtained from the perspective of artificial intelligence or bionics through extensive experiments. The move-to-goal behavior is a typical point-to-point (PTP) control algorithm, which steers the robotic fish to move from an initial point to a goal point by adjusting its orientation and speed continuously according to real-time visual feedback. The avoid-obstacle behavior based on APF can be expressed as follows:

$$\theta = \begin{cases} \phi, & (L < M_{min}) \cap (R < M_{min}) \\ \theta_0, & L \leq R \\ -\theta_0, & L > R \end{cases} \quad (5)$$

$$v = \begin{cases} \phi, & (L < M_{min}) \cap (R < M_{min}) \\ 0, & (L > M_{max}) \cup (R > M_{max}) \\ v_{max}, & other \end{cases} \quad (6)$$

where θ and v are the outputs of avoid-obstacle behavior, θ determines the desired direction of the robotic fish, v denotes the desired speed of the robotic fish, ϕ means the output of move-to-goal behavior in the case of no obstacles, θ_0 represents the orientation angle to avoid the closer obstacle on one side, v_{max} represents the maximum swimming speed, L and R are used to indicate the present distances of the

robotic fish to the obstacles on its left side and right side respectively, M_{min} means the case without regard to the obstacles, and M_{max} means the case that the robotic fish is very close to the obstacle. The parameters can be obtained as follows:

$$L = \frac{1}{\sqrt{d_{camera}^2 + \Delta x_l^2 + m_0}} \quad (7)$$

$$R = \frac{1}{\sqrt{d_{camera}^2 + \Delta x_r^2 + m_0}}$$

$$M_{min} = \frac{1}{d_{range} + m_0} \quad (8)$$

$$M_{max} = \frac{1}{v \Delta t + m_0}$$

where d_{camera} denotes the vertical distance of the robotic fish to the obstacle measured through the captured image of the onboard camera in real time (see Section IV), Δx_l represents the error value in the image's x-axis between the center of the image frame and the centroid of the obstacle region on the left side, Δx_r for the obstacle on the right side, d_{range} denotes the biggest distance that can be detected and measured from the camera, and m_0 is a gain value.

VI. EXPERIMENTS AND RESULTS

In this section, the experimental results of the water-polo-attacking are presented. The experiment results are given in two aspects: pictures and videos.

The efficiency of the proposed control algorithms is tested in several experimental trials. It has been observed that even starting from the same initial states including initial positions of the robotic fish and the water polo, the attacking tasks consume different amounts of time to finish and the autonomous robotic fish carries out different sequences of actions. This is because there are more uncertainties in underwater manipulation than in ground operation. A very small disturbance might be enlarged by the liquid medium and result in different recognitions leading to different action sequences for the robotic fish. Although the experimental results are not perfect, they are still successful and promising.

Fig. 7 illustrates a water-polo-attacking experiment which has high efficiency and succeeds within 17 s. In this experiment, the cylinder-shaped obstacle is located at one corner of the tank, the cubic obstacle stands in the center, the robotic fish starts from opposite side of the goal, and the water polo is set approximately in the center. Fig. 8 shows the trajectories (extracted from corresponding video clip) of both the robotic fish and the water polo, which partially validate the feasibility of the proposed control algorithms.

VII. CONCLUSIONS AND FUTURE WORKS

This paper first presents the development of an autonomous robotic fish and then concentrates on its application in a water-polo-attacking task. Considering the characteristics of the robotic fish and the hydro-environment, an artificial potential field approach was adopted for path planning and obstacle avoidance. Corresponding experimental results show the effectiveness of the proposed control algorithms. Water-polo-attacking is really a novel task that might be an extended competition of RoboCup in underwater

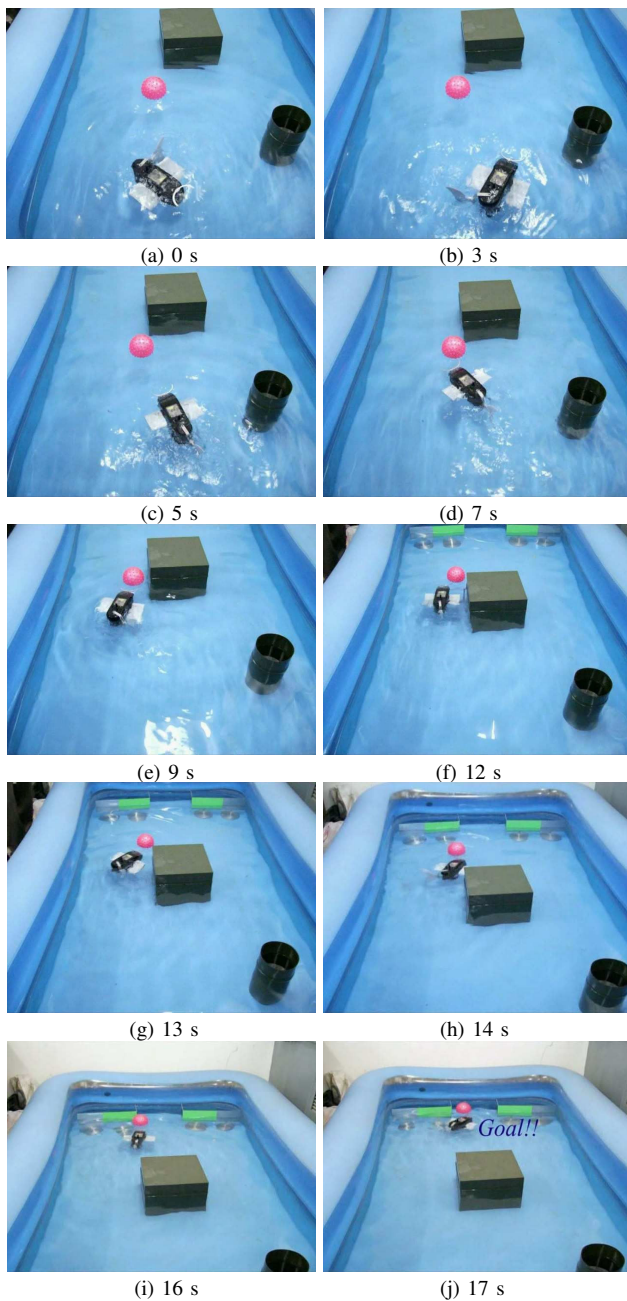


Fig. 7. Image sequence of water-polo-attacking of the autonomous robotic fish. Water-polo-searching [from (a) to (b)], water-polo-pushing [from (c) to (d)], obstacle-avoiding [from (e) to (h)], and shooting [from (i) to (j)].

environment. The ongoing and future work will focus on the control strategies of multiple robotic fish in a cooperative water-polo competition. Role assignments will be introduced for attacker and blocker. Eventually, a competition platform for multiple robotic fish is planned to be established in the future, namely RoboFish-Cup.

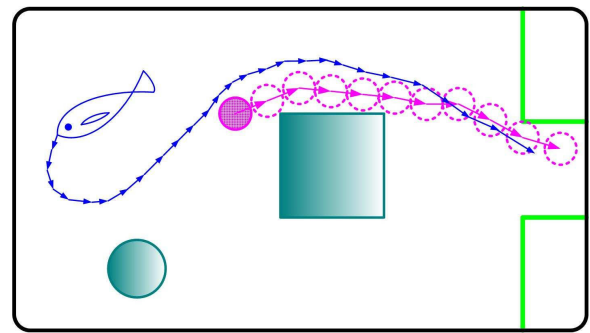


Fig. 8. Experimental trajectories of the robotic fish and the water polo estimated from the corresponding video.

REFERENCES

- [1] M. S. Triantafyllou, and G. S. Triantafyllou, "An efficient swimming machine", *Sci. Amer.*, vol. 272, no. 3, 1995, pp. 64-70.
- [2] D. Barrett, M. Grosenbaugh, and M. Triantafyllou, "The optimal control of a flexible hull robotic undersea vehicle propelled by an oscillating foil", in *Proc. IEEE AUV Symposium*, 1996, pp. 1-9.
- [3] R. Mason, and J. Burdick, "Experiments in carangiform robotic fish locomotion", in *Proc. Int. Conf. Robotic Automation*, 2000, pp. 428-435.
- [4] J. Liu, H. Hu, and D. Gu, "A hybrid control architecture for autonomous robotic fish", in *Proc. Int. Conf. Intelligent Robots and Systems*, 2006, pp. 312-317.
- [5] N. Kato, "Control performance in the horizontal plane of a fish robot with mechanical fins", *IEEE J. Oceanic Eng.*, vol. 25, no. 1, 2000, pp. 121-129.
- [6] F. Delcomyn, "Neural basis for rhythmic behaviour in animals", *Science*, vol. 210, 1980, pp. 492-498.
- [7] J. Buchanan, S. Grillner, "Newly identified 'glutamate interneurons' and their role in locomotion in the lamprey spinal cord", *Science*, vol. 236, 1987, pp. 312-314.
- [8] S. Grillner, P. Wallen, and L. Brodin, "Neuronal network generating loco- motor behavior in lamprey: Circuitry, transmitters, membrane properties, and simulation", *Annual Review of Neuroscience*, vol. 14, 1991, pp. 169-199.
- [9] M. Sfakiotakis, D. M. Lane, and J. B. C. Davies, "Review of fish swimming modes for aquatic locomotion", *IEEE J. Oceanic Eng.*, vol. 24, 1999, pp. 237-252.
- [10] S. Lenser, J. Bruce, M. Veloso, "CMPack: A complete software system for autonomous legged soccer robots", in *Proceedings of the Fifth International Conference on Autonomous Agents*, May 2001.
- [11] J. Bruce, T. Balch, and M. Veloso, "Fast and inexpensive color image segmentation for interactive robots", in *Proc. IEEE/RSJ Int. Conf. Intelligent Rob. and Sys.*, Oct. 2000, pp. 2061-2066.
- [12] J. Fasola and M. Veloso, "Real-time object detection using segmented and grayscale images", in *Proc. IEEE Int. Conf. Robotics and Automation*, May. 2006, pp. 4088-4093.
- [13] O. Khatib, "Real-time obstacle avoidance for manipulators and mobile robots", *Int. J. Robotics Research*, vol. 5, no. 1, 1986, pp. 90-98.
- [14] P. Huang, P. Yang, and Z. liu, "Robot soccer path planning research based on predictive artificial potential field", in *Proceedings of the 5th World Congress on Intelligent Control and Automation*, June 15-19, 2004, pp. 868-870.
- [15] Q. Cao, Y. Huang, J. Zhou, "An evolutionary artificial potential field algorithm for dynamic path planning of mobile robot", in *Proc. IEEE/RSJ Int. Conf. Intelligent Rob. and Sys.*, Oct. 2006, pp. 3331-3336.